Computational Study of Recirculating Flows Induced by Axial Swirler

Muthu selvan G[#], Muralidhara H S[#], Surya J[*], Dinesh Kanth T.P[#]
[#] Propulsion Division, CSIR - National Aerospace Laboratories, Bangalore,India
[1] mechmuthu1@nal.res.in
[2] murali@nal.res.in
[4] dineshkanthtp@gmail.com
[*] Mohammed Sathak Engineering College, Kilakarai, Tamil Nadu.
[3] surya3848@gmail.com

Abstract: **The present work reports a computational study of flow through axial swirler for various swirl angles from 20^0 to 70^0 in steps of 10^0. Three dimensional flow through the axial swirler have been simulated by means of computational fluid dynamics (CFD) using the code Ansys – Fluent 13. The objective of this work is to understand the flow field characteristics downstream of the swirler at different axial locations and to find length and width of Central Toroidal Recirculation Zone (CTRZ) for all six cases of swirler. The recirculation velocities at the centre and corner regions are well captured by solving the appropriate governing equations, namely, conservation of mass and momentum using the SIMPLE algorithm. Turbulence has been modelled using Reynolds Stress Model. The numerical predication of mass flow rate has been compared with experimental correlation. It has been observed that, good agreement is obtained between numerical predication and the experimental correlation.**

Keywords---- Swirler, swirl angle, Recirculating Flows, Central toroidal recirculation zone, Reynolds stress model.

Nomenclature

D_h	- Hub diameter
D	- Tip diameter
α	- Swirl angle
S_N	- Swirl Number
L	- Length of Central Toroidal Recirculation Zone
W	- Width of Central Toroidal Recirculation Zone
M	- Location at which recirculation zone has maximum width
Z	- Distance along axial direction of domain
K	- Swirler Constant
m	- Mass flow rate through swirler
A_{sw}	- Inlet area of swirler
A_L	- Confinement area
ΔP	- Pressure drop across swirler
ρ	- Air density at inlet of swirler
CTRZ	- Central Toroidal Recirculation Zone
CRZ	- Corner Recirculation Zone
LDV	- Laser Doppler Velocimetry system
LDA	- Laser Doppler Anemometry
PIV	- Particle Image Velocimetry
NO_X	- Oxide of nitrogen emissions
CO	- Carbon mono oxide
RSM	- Reynolds Strees Model

Introduction:

Producing strong swirl in aero and industrial gas turbine combustor is essential in order to assist in flame stabilization of the high intensity combustion and low emission. The degree of the swirl applied to the flow affect the flame size, shape and stability as well as the combustion efficiency. For an axial swirler having a uniform swirl angle, the swirl number is related to the swirl angle, hub diameter and tip diameter as given by equation (1)

$$S_N = \frac{2}{3}\frac{[1-(D_h/D)^3]}{[1-(D_h/D)^2]}(tan\alpha) \quad \text{----- (1)}$$

When rotating motion is imparted to a fluid by vanes of swirler, the fluid flow emerging from the swirler has a tangential velocity component in addition to the axial and radial components of velocity encountered in non swirling jets. The presence of the swirl results in the setting up of radial and axial pressure gradients which, in turn influence the flow field. In the case of strong swirl, the adverse axial pressure gradient is sufficiently large to result in reverse flow along the axis and the setting up of an internal recirculation zone. This recirculation zone, which has the form of a toroidal vortex, plays an important role in the flame stabilisation, as it constitutes a well-mixed zone of combustion products and acts as a storage of heat and of chemically active species located in the centre of the jet near the burner exit. The recirculation zone ends at stagnation point. After stagnation point the reverse axial velocity disappears and the peak of the axial velocity profile shifted towards the centre line as the effect of the swirler diminishes. The recirculation in the swirling flow is closely related to the inlet flow conditions such as inlet pressure, inlet velocity, swirl number, and the upstream and downstream conditions. The effect of these factors on the swirling flow field shows that the flame stability and mixing quality can be improved by increasing the inlet conditions. This recirculation zone size and shape can influence residence time of fresh air-fuel mixture entering into the primary zone of combustor, and as a result NO_x production. Therefore proper selection of a swirler is needed to reduce NO_x formation.

The effects of swirl on flow field and combustion have been extensively investigated by various people. Beer and Chigier classified (1972) the swirling flow into two regions; weak swirling flow ($S_N < 0.6$) and strong swirling flow ($S_N > 0.6$). In weak swirling flow, the axial pressure gradients are insufficient to cause internal recirculation. In strong swirling flow, the axial pressure gradients are sufficiently large to cause internal recirculation. Syred (1971) measured the spatial distributions of the mean temperature and velocity for combustion in recirculation zones using thermocouple and hot wire anemometer. Their experimental results showed that aerodynamics forces were so dominant that little change occurs to flow field as a result of chemical reaction in the flame in the strong swirl conditions. Shape and size of recirculation zone and reversed mass flow rate were only slightly reduced under combustion conditions as compared with isothermal conditions. Kilik (1985) demonstrated the effect of swirl angle and blockage ratio on the aerodynamics characteristics of the downstream recirculation region and the pressure drop through the swirler. He also compared the effect of flat and curved vanes on the efficiency of swirl generation and found that the pressure loss through a swirler can be reduced over 50% by using curved vanes for the same angle and blockage ratio. Ahamed and Nejad (1992) presented detailed measurements on the confined isothermal, swirling flow field by using two component Laser Doppler Velocimetry (LDV) systems. Bulzan (1995) presented the LDA measurement of the structure of a swirl stabilized, reacting spray. Gas phase axial velocity is increased for the combusting spray case as compared with the single-phase isothermal case because of the gas expansion caused by heat release. The strength of the recirculation zone is increased for the reacting case and the overall length recirculation is shorter as compared with single phase case. Sheen (1996) conducted the velocity measurement for the unconfined annular swirling jet flows with several Reynolds number and swirl number by using LDV system. He concluded that the recirculation zones could be classified into several typical flow patterns: stable flow, vortex shedding, transition penetration vortex breakdown and attachment. V.Ganesan (2004) reported results from the computational work done with four different axial swirler, wall static pressure and axial velocity distribution. From the studies it was concluded that RSM turbulence model were able to handle swirling flows accurately, especially swirls caused by high swirl angles. Panduranga Reddy and S.R Chakravarthy (2006) investigated the flow field characteristics of a gas turbine swirler on a model combustion chamber, using PIV. They demonstrated the effect of pressure drop on the recirculation zone, as the pressure drop reduces from 0.1 to 0.05 bar the length of (CTRZ) has been varied from 4D to 3D. Thundi karuppu Raj and Ganesan (2009) reported results from the experimental study on flow through 8 blade 30^o swirler, made axial velocity measurement along the entire length of model at different stations using five-hole Pitot probe. The recirculating axial velocity distribution with in the CTRZ and out of CTRZ was well captured. After the CTRZ reverse axial velocity disappears and the peak of the axial velocity profile shifted towards the centre line as the effect of the swirler diminishes. Mohamad Shaiful Ashrul Ishak (2005) studied the effect of swirl number on emissions. Eight different swirler cases were selected for their experimental study. From their results it was considered that the NO_X reduction of more than 26 percent was obtained at equivalence ratio 0.83 for swirl number of 1.427 compared to 0.046, CO emissions were reduced by 48 percent in 1.911 compared to 0.046.

Objectives

The main objectives of the present study are:

1. To predict the flow through a axial swirler
2. To study the effects of swirl angle on the mass flow rate through swirler
3. To study the effect of swirl angle on the length and width of CTRZ.
4. To study the effect of swirl angle on axial velocity distribution along the axial and radial directions with in the CTRZ and out of CTRZ

Computational domain:

The geometry under consideration for the present study is shown in figure – 1. This simplified model consists of an inlet pipe of length 100mm and the diameter of 26mm and swirler is fixed with inlet pipe. Swirler consists of 8 vanes of thickness 1mm and height of 5mm. All the eight vanes are symmetrical about centre axis. A divergent extension was provided at the swirler exit to support of the strength of tangential velocity produced by swirler, with inner diameter 26mm and outer diameter 90mm. A long square duct consist of 100*100 mm and length is about 600mm fixed with dome exit, further a convergent type nozzle was attached to prevent any flow reversal of flow from the atmosphere into the chamber.

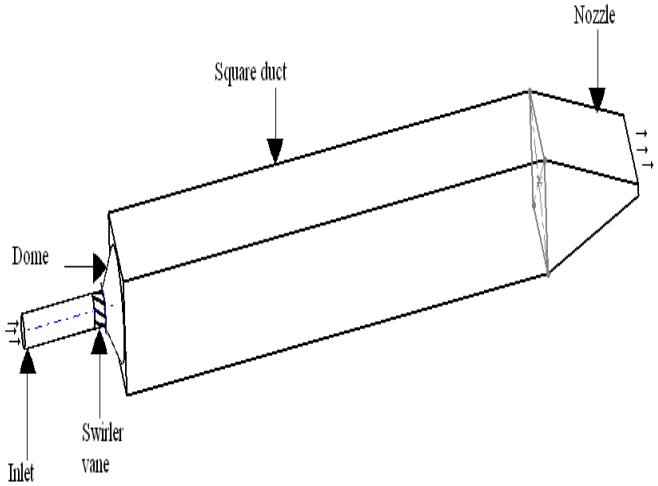

Figure – 1 Schematic diagram of computational domain

Assumptions and boundary conditions

Six different cases of swirler (20^o, 30^o, 40^o, 50^o, 60^o and 70^o) were taken for this study as mentioned in table - 1 with corresponding swirl number. The flow is assumed to be steady, isothermal and turbulent. The inlet boundary condition chosen is pressure inlet and given fixed value of about 1.5bar, temperature 300K, hydraulic diameter 26mm and turbulent intensity of 1% was given. At the exit, pressure outlet boundary was chosen and given fixed value of 1 bar, temperature 300K, hydraulic diameter 35.68 mm with turbulent intensity of 5%. Reynolds stress model was used to capture turbulence.

Swirl angle	20 °	30 °	40 °	50 °	60 °	70 °
Swirler number	0.299	0.474	0.689	0.979	1.423	2.258

Table – 1 The swirl number for different swirler cases

Geometry and grid generation

Swirler with appropriate vane angle and flow region as shown in figure - 1 modelled using solid works software. Three dimensional unstructured grid was generated using tetrahedral mesh in Ansys work bench. The grid generated swirler model used for this analysis is shown in the figure – 2. The number of grid cells lies between 391669 cells to 393495 cells depending upon the swirl angle. Cells were refined in the critical regions, like swirler inlet and exit, in anticipation of high velocity and pressure gradient. Grid independent tests were conducted to ascertain the adequacy of grid and it was found that, grid distribution used was quite adequate. The grid of computational domain used for this analysis is shown in the figure – 3.

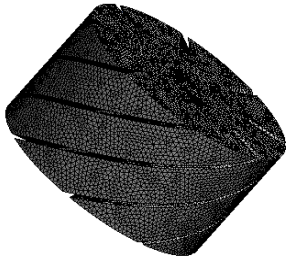

Figure – 2 Computational grid of axial Swirler

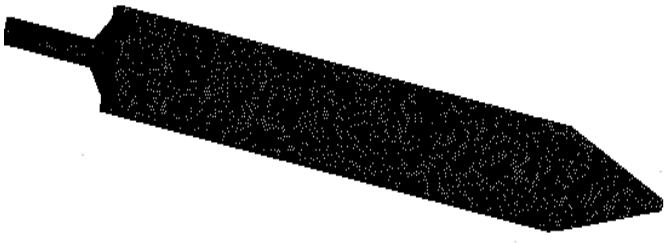

Figure – 3 Computational grid of domain

Results and discussion

1. Swirling flow field

Figure -4 presents swirling flow field generated by 30^o axial swirler , in that axial velocity contour within the range of recirculation zone (-1 to +1 m/s) was superimposed over velocity vector field for a better understanding of recirculation zone formation. The length (L) and width (W) of recirculation zone considered in this study and the location at which the CTRZ has maximum width (M) is also shown in the figure - 4. From the maximum width to stagnation point the reverse flow axial velocity gradually reduces to zero. After stagnation point the reverse axial velocity disappears and forward axial velocity profile was formed. The corner recirculation zone present near the walls of square section and on dome also well captured. The velocity vector plots at four different axial locations are shown in the figure – 5. First axial location shows forward axial velocity of the flow at swirler exit, also it shows corner recirculation zone present near the dome exit. Second axial location shows a strong outward radially expanding swirl flow at the center, straight flow near the walls of the domain. At the center it also shows the reverse axial flow towards swirler exit. Third axial location shows a smaller central vorticity zone compare to second axial location and it also shows straight flow near the walls of the domain. Fourth plane located after stagnation point of the flow shows forward axial velocity profile, since after recirculation zone the reverse axial velocity disappears and the peak of the axial velocity profile shifted towards the centre line as the effect of the swirler diminishes.

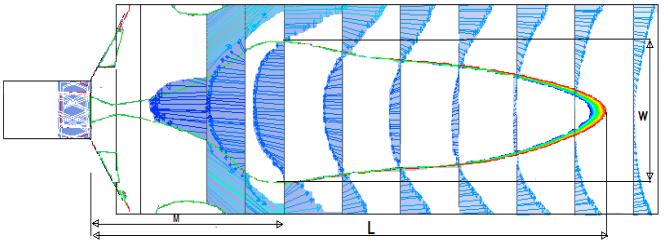

Figure – 4 The structure of central toroidal recirculation zone.

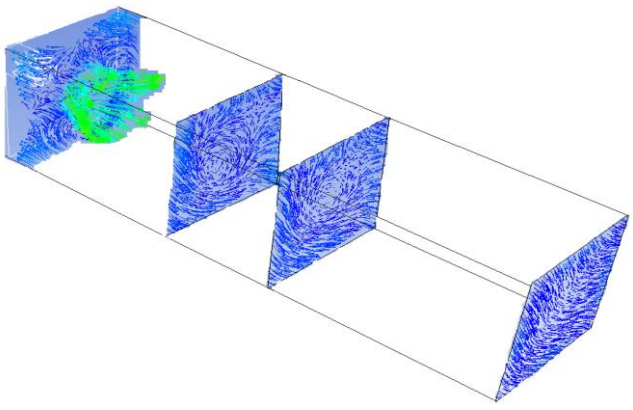

Figure – 5 Velocity vector plot at different axial locations

2. Mass flow rate

Computational study performed for all the six cases of swirler for constant pressure drop of 0.5bar. Figure – 6 shows mass flow rate through different cases of swirler at a constant pressure drop across the domain against swirl angle. As the swirl angle increases the mass flow rate through swirler reduces, since higher swirl angle provides larger aerodynamic resistance to the flow. The calculated values of mass flow rate through CFD analysis were compared with experimental correlation provided by Knight.M.A and Walker.R.B (1957). In the experimental correlation the mass flow rate is related to the swirler area, pressure drop across the swirler and swirl angle as given by equation (2). The CFD results matches with the experimental correlation values.

$$m = \left\{ \frac{2\rho\Delta P}{K\{(\sec\ \alpha/A_{SW})^2 - (1/A_L)^2\}} \right\}^{0.5} \quad \text{----- (2)}$$

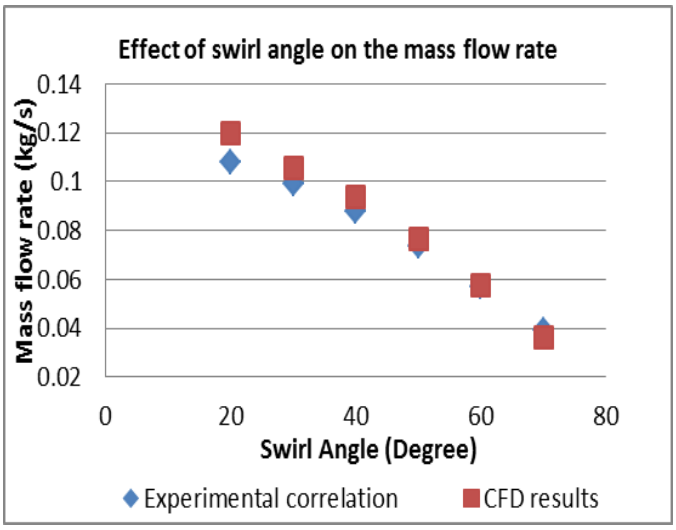

Figure – 6 Mass flow rate through axial swirler of all six cases.

3. Size of the recirculation zone

Figure - 7 shows the contours of CTRZ produced by all six cases of axial swirler. The swirler with swirl angle 20° (S_N = 0.299) produces a detached recirculation zone and bigger Corner Recirculation Zone (CRZ), since it was not able to convert considerable amount of axial velocity to tangential component, so it produces comparatively higher axial velocity at the swirler exit. Because of this higher axial velocity at the swirler exit, the flow pushes further downstream and forms detached CTRZ and bigger CRZ. The swirler with swirl angle 30° (S_N = 0.474) produces slightly an attached recirculation zone with neck formation, and smaller corner recirculation zone, since this also produces higher axial velocity at swirler exit. The swirler with swirl angle 40° (S_N = 0.689) produces an attached recirculation zone, but shows a step in CTRZ. The swirler with swirl angle 50° (S_N = 0.979) also produces an attached recirculation zone with same kind of step in CTRZ. As the swirl angle increase further the swirler produces recirculation without step. Size of CRZ diminishes with swirl angle. This corner recirculation present in the gas turbine combustor will act as a source of NO_x formation as it provides localized high temperature region. So increase in swirl intensity will suppress the NO_x formation in the combustor.

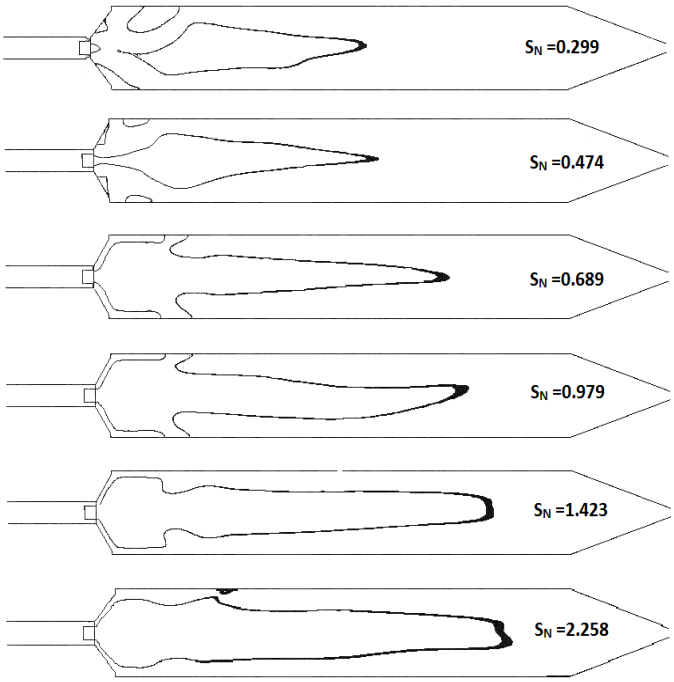

Figure – 7 Central Toroidal Recirculation Zone of all six cases.

The length and width of CTRZ taken from the CFD analysis mentioned in the table – 2. The location at which CTRZ has maximum width also was mentioned in the table – 2. Length of CTRZ plotted against swirl angle in the figure – 8, it shows that length of CTRZ increases with swirl angle initially, but after 50 ° it is almost maintained constant. Width of CTRZ plotted against swirl angle in the figure – 9, it indicates that, increase in swirl angle does not affect the width of CTRZ. The location of maximum width of CTRZ plotted against swirl angle in the figure – 10, as the swirl angle increases maximum width moves towards swirler exit and diminishes the CRZ.

Swirl angle	Length of CTRZ(L/D)	Width of CTRZ (W/D)	Location of Maximum width (M/D)
20 °	13.61	2.12	6.15
30 °	14.23	3.07	5.38
40 °	17.80	3.07	2.30
50 °	19.03	3.07	1.92
60 °	20.15	3.23	1.73
70 °	20.19	3.23	1.73

Table – 2 The approximate length scales of the CTRZ and CRZ obtained in the midplane of all the six cases of swirler for the pressure drop of 0.5 bar.

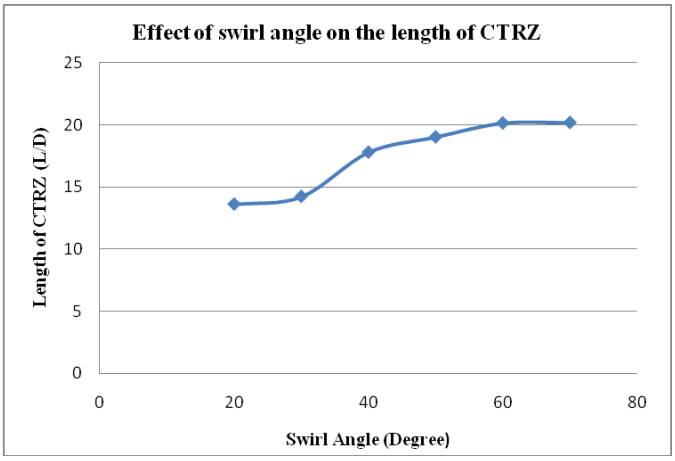

Figure – 8 Length of CTRZ of all six cases of swirler

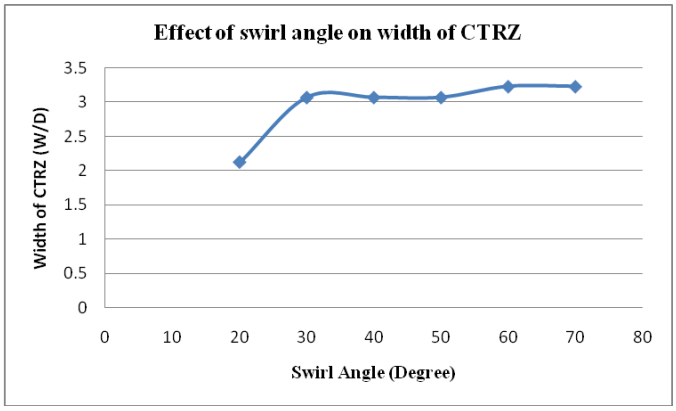

Figure – 9 Width of CTRZ of all six cases of swirler

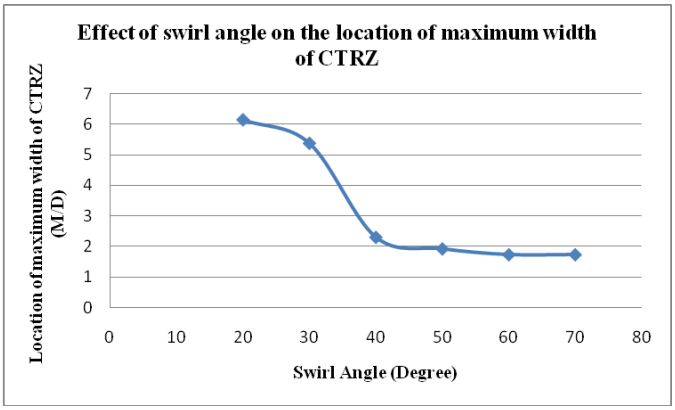

Figure – 10 Location of maximum width of CTRZ of all six cases of swirler

4. Axial velocity distribution

Axial velocity distributions of all six cases of swirler along the axial direction are shown in the figure – 11, it indicates that reverse flow axial velocity with in the recirculation zone reduces with increase in swirl angle. It has been observed that 30^o swirler has higher reverse flow axial velocity with in the recirculation zone compare to all other cases while 20^o swirler produces forward axial velocity at the exit, and gradually reduces to negative axial velocity and forms CTRZ. This profile matches with 20^o case of figure – 7.

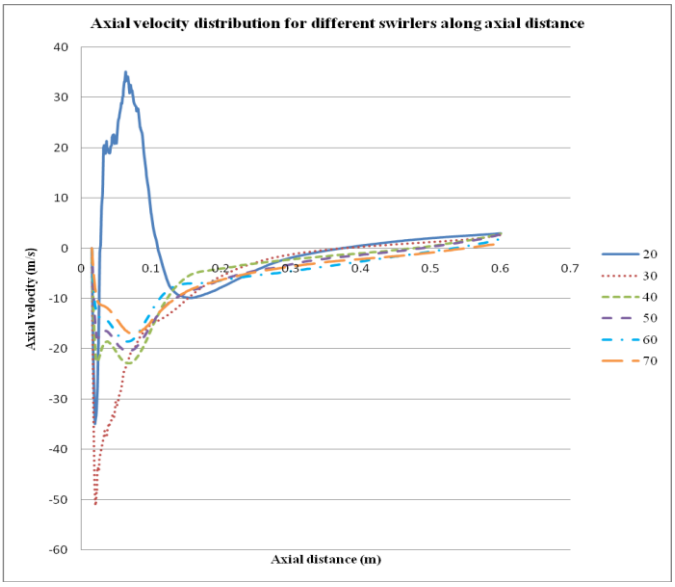

Figure – 11 Axial velocity distribution along axial distance of all six cases.

Axial velocity distributions of all six cases of swirler along the radial direction are plotted at four different axial locations (Z/D = 0.769, 1.538, 6.153 and 15.384) in the figure – 12. It shows that 20^o case has similar axial velocity profile as 30^o case at Z/D = 0.769 downstream of the swirler exit. Their axial distributions show a double hump-type velocity profile. But 30^o shows very narrow reverse flow at the centre of the domain, this narrow reverse flow was responsible for neck formation in the CTRZ of 30^o case, as mentioned in figure – 7. But 20^o case does not show any reverse flow at Z/D = 0.769. For the 40^o, 50^o, 60^o and 70^o cases, the values of axial velocities are negative near the swirler exit at Z/D = 0.769. This indicates the presence of recirculation zone for these cases near the swirler exit as shown in the figure – 7. From Z/D = 0.769 to Z/D = 1.538 the axial velocity decay very fast for weak swirl cases (20^o, 30^o). The 20^o case shows some reverse flow velocity at Z/D = 1.538, from this axial location onwards 20^o case form recirculation zone. For the stronger swirl cases, the CTRZ becomes wider and peak axial velocities were almost same. At the axial location of Z/D = 6.153, all the cases shows similar reverse flow velocity profile. Weak swirler cases (20^o, 30^o) show higher peak reverse flow velocities than stronger cases, this is matches with figure – 11. Weak swirler cases (20^o, 30^o) show higher peak forward flow velocities at the edge of CTRZ than stronger. At axial location of Z/D = 15.384, the axial velocity for the weak cases decay so fast that these cases show forward axial velocity profiles, so recirculation zone ends before this location for weak cases as mentioned in the table - 2. The strong swirl cases still have negative axial velocities at these positions, since this axial location lies within the recirculation zones

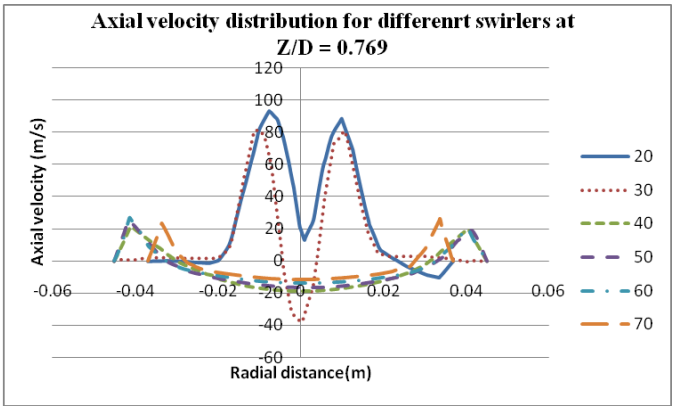

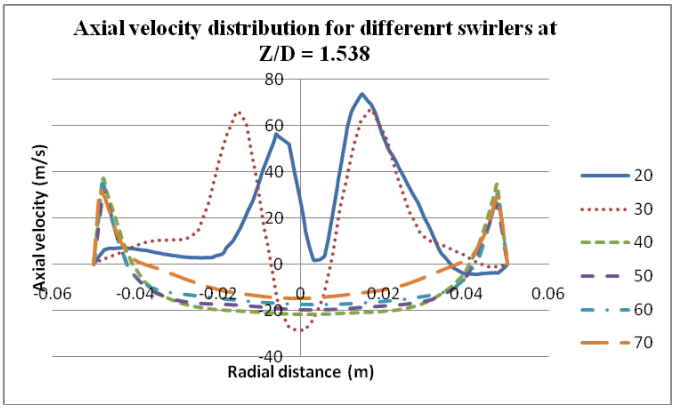

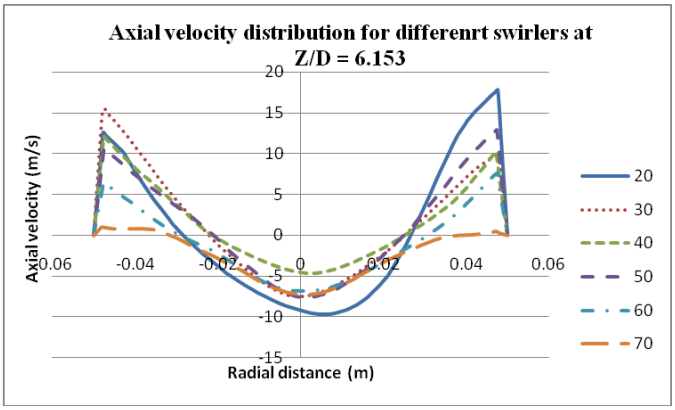

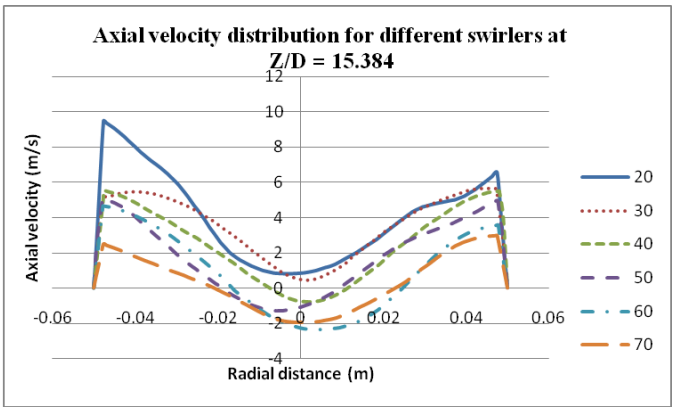

Figure – 12 Axial velocity distribution along radial distance of all six cases.

Conclusions

From the study of swirler with different swirl angle the following conclusions were made.

1. Mass flow rate through the swirler reduces with increase in swirl angle, matches with results of experimental correlation provided by Knight.M.A and Walker.R.B.
2. The length of CTRZ increases with swirl angle initially, but after 50^{o} it is almost maintained constant.
3. The corner recirculation zone diminishes with increase in swirl angle,The location, at which CTRZ has maximum width reduces with swirl angle initially, but remains constant after 60^{o} swirler.

Reference

1. Beer, JM and Chigier, N.A., Combustion Aerodynamics," Applied Science Publisher LTD, London 1972.
2. Syred, N., Chigier, N.A and Beer, J.M., "Flame stabilization in recirculation zones of jets with swirl", 13th symposium on Combustion, The Combustion Institute, Pittsburgh, PA, pp.617-624,1971
3. Kilik, E., "Influence of the Blockage Ratio on the efficiency of Swirl Generation with vane swirlers," AIAA Paper 85-1103,21th Joint Propulsion Conference, Monterey, CA 1985
4. Ahmed, S.A., and Nejad, A.S., "Velocity Measurements in a Research Combustor. Part I. Isothermal Swirling Flow," Experimental Thermal and Fluid Science Journal, Vol.5, pp.162-174, 1992
5. Bulzan, D.L., "Structures of a Swirl Stablized Combusting Spray," Journal of Propulsion and power, Vol, 11, No.6.pp.1093-1102, 1995.
6. Sheen, H.J.,Chen,W.J., and Jeng,S.Y., " Recirculation Zones of Unconfined and Confined Annular Swirling Jets," AIAA Journal, Vol.34, No3,pp.572-579, 1996.
7. S.Bharath Krishna, Prof V.Ganesan CFD analysis of flow through Vane Swirlers. Journal of the Institution of Mechanical engineering. (India). 2004.
8. Panduranga Reddy, R.I. Sujith and S.R. Chakravarthy, "Swirler Flow Field Characteristics in a sudden Expansion Combustor Geometry" Journal Of propulsion And Power Vol.22.No.4.july-August 2006
9. R.Thundi karuppu Raj & V.Ganesan "Experimental Study Of recirculating Flows Induced by vane Swirler Indian Jounal of Engineering & material science vol.16,February 2009,pp.14-22
10. Mohamed Shaiful Ashrul Ishak Mohammad nazri Mohd jaffar " The Effect of Swirl number on Reducing Emmision From Liguid Fuel Burner system" Journal mechanical June 2005,No.19,48-56
11. Knight.M.A and Walker.R.B, " The Component Pressure Losses in Combustion Chambers," Aeronautical Research Council R and M 2987, England 1957